PETROPHYSICS. VOL. 45. NO. 6 (NOVEMBER-DECEMBER 2004): P. 530–539; 9 FIGURES

Technical Note

Correcting for Tool Decentralization of Oriented Six-Arm Caliper Logs for Determination of Contemporary Tectonic Stress Orientation

D. Wagner,[1] B. Müller,[1] and M. Tingay[1]

ABSTRACT

Tool decentralization is a major problem in the analysis of six-arm caliper data, particularly in highly deviated wells. It precludes accurate determination of borehole geometry and hence, interpretation of borehole volume, stratigraphic horizons and present-day stress orientation. We test four methods for correcting tool decentralization of six-arm caliper data, for the primary purpose of interpreting present-day stress orientations from borehole breakouts. The 'chord approach' and 'ellipse algorithm' yielded the most accurate corrections for tool decentralization in real and modeled scenarios of breakouts, key-seats and in-gauge holes.

INTRODUCTION

Knowledge of the present-day stress orientation is becoming increasingly important to the petroleum industry in order to resolve problems of borehole stability (Peska and Zoback, 1995), hydraulic fracturing (Shlyapobersky and Chudnovsky, 1994) and sub-surface fluid flow (Sibson, 1994). Present-day stress orientation in oil fields is commonly determined from borehole features, such as breakouts interpreted from four-arm caliper data and resistivity or acoustic image logs (Gough and Bell, 1982; Plumb and Hickman, 1985; Barton, 1988). Six-arm caliper data can also be used for stress analysis and, indeed, has several advantages over four-arm caliper data, but is very rarely used due to problems of tool decentralization (Jarosinski, 1998). Four-arm caliper tools remain centered in the borehole by means of two orthogonal pairs of coupled caliper arms that measure the borehole diameter. However, the caliper arms on the six-arm tool are independently hinged, so that arm extension is not balanced on either side of the tool and tool decentralization can occur (Figure 1). Determination of borehole geometry becomes more complicated if the six-arm caliper tool is decentralized, especially in highly deviated or non-circular wells, such as in zones of breakouts or key-seats. This paper tests four techniques for correcting tool decentralization and ascertaining borehole geometry on real and synthetic six-arm caliper data, thus providing an alternative means for analyzing present-day stress orientations in the oil patch.

Interpretation of breakouts from six-arm caliper data

Borehole breakouts are stress-induced, generally symmetrical borehole elongations with their long axis perpendicular to the maximum horizontal stress orientation (Kirsch, 1898; Plumb and Hickman, 1985). However, especially on caliper log data, breakouts can be confused with other borehole elongations such as key-seats and washouts. Key-seats are asymmetric drilling-induced enlargements of the original circular borehole and usually occur on the high or low side of the borehole. Washouts are irregular borehole enlargements in all directions caused by sloughing of mate-

Manuscript received by the Editor December 12, 2003, and the revised manuscript was received August 4, 2004.
[1]World Stress Map Project, Heidelberg Academy of Sciences and Humanities, Geophysical Institute, University of Karlsruhe, Hertzstrasse 16, 76187 Karlsruhe, Germany

rial from the borehole wall. Breakouts can be directly interpreted from image logs or by means of a strict set of criteria from four-arm caliper data (Plumb and Hickman, 1985; Bell, 1990; Zajac and Stock, 1997). The rules governing breakout interpretation from four-arm caliper logs allow the interpreter to examine the change in borehole shape over depth, but these rules require the tool to be centered in the borehole. Possible tool decentralization of the six-arm caliper tool precludes using the rules for breakout interpretation. However, correcting for tool decentralization allows all pad positions at all depths to be determined relative to a common point (the center of the borehole). Hence, all pad positions over a suspected breakout interval can be overlaid ('stacked') to better ascertain the overall borehole shape and thus the stress orientation.

REFERENCE COORDINATE SYSTEM

There have been only a few studies on correcting tool decentralization or performing breakout analysis from six-arm caliper data (Figure 1). Zajac and Stock (1997) described methods to calculate the breakout elongation direction from six-arm caliper data, but without considering tool decentralization problems. Jarosinski (1998) calculated the tool-offset based on the assumption that the circular borehole axis is located near the 'center of mass' of the hexagon formed by the pads of the six-arm tool at the borehole wall. Although very few decentralization correction methods have been tested for the six-arm caliper tool, several other six-arm tools exist that can also suffer from decentralization. Schlumberger obtains the position of its six-arm Environmental Measurement Sonde using a best-fit ellipse algorithm and estimates the tool arm positions that would be obtained from a four-arm caliper measurement. A number of tool decentralization corrections have been used on borehole televiewer data: the center of mass method and the circle algorithm in circular wells (Bässler, 1995), and the ellipse algorithm in elliptical boreholes (Lysne, 1986; Barton, 1988; Bässler, 1995).

The decentralization correction methods outlined above are normally applied in a quasi-automatic way, where breakout orientation is calculated as the average 'long-axis' direction over a specified depth range. Due to the lack of visual control in this technique, key-seats or washouts may be wrongly interpreted as breakouts, and we suggest visually confirming all interpreted breakout zones.

Reference Coordinate System

The tool position (x_0, y_0) is calculated in a Cartesian coordinate system with respect to this center. The measured caliper lengths (P_i) of the individual pads and pad orientations are given in a coordinate system with its origin at the center of the tool. The reference azimuth of pad 1 is φ_1, given clockwise from north (Figure 1). Due to tool construction, the other pad azimuths are at

$$\theta_i = \theta - (i-1)\cdot 60°, \theta = 90° - \varphi_i \text{ with } i = 1,\ldots,6. \quad (1)$$

θ_i is measured anti-clockwise from the x'-axis of the tool system (Figure 1). In the borehole coordinate system, the pad positions fulfil

$$R_i^2 = [x_0 + P_i \cos\theta_i]^2 + [y_0 + P_i \sin\theta_i]^2, \quad (2)$$

where R_i is the distance from the borehole center to the pad P_i and equals half the bit size in perfectly circular boreholes. The angular differences between the angles β_i in the borehole coordinate system differ from 60°, whereas the angular differences are equal (60°) in the tool coordinate system (Figure 1). The corresponding angles β_i are

$$\beta_i = \arctan\frac{y_0 + P_i \sin\theta_i}{x_0 + P_i \cos\theta_i}. \quad (3)$$

Circle Algorithm

The 'circle algorithm' enables the calculation of both the center of a circle and its radius (Bässler, 1995). The basic geometrical theorem is that any three points in a plane that

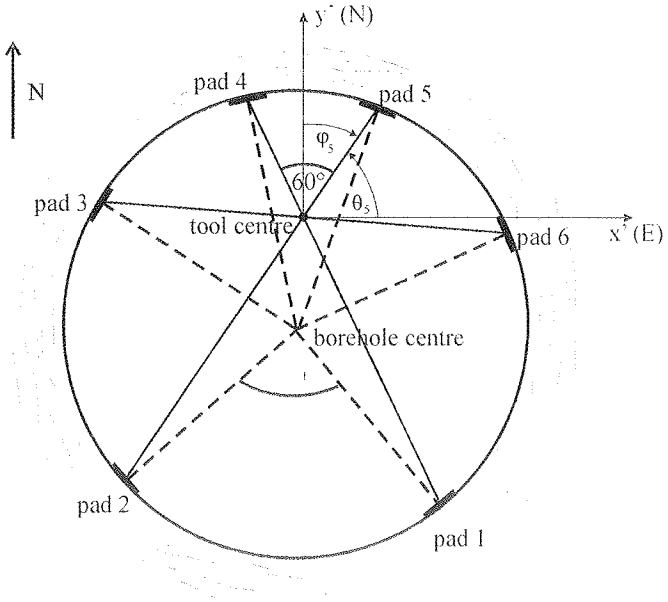

FIG. 1 A decentralized tool in a circular borehole. The caliper arms have different lengths but equal angular differences of 60°. However, the distance values are equal (dotted lines), but the angles between the caliper arms differ from 60° when measured from the borehole center. θ = azimuth of the reference pad. For further explanation, see the text.

are not in a straight line define a unique circle. There are six measured pad values $P_1,\ldots, P_6$ available, and any combination of three of them determines the center point of the circumscribed circle of radius r (the smallest circle that encloses the three points). The lines connecting the three points are chords of the circumscribed circle and form the sides of a triangle. The perpendicular bisectors of these lines intersect at the center of the circumscribed circle.

With the origin of the coordinate system at the center of a circle with radius r; any point with coordinates (x_i, y_i) on the circle obeys $r^2 = x_i^2 + y_i^2$. If the tool is at the location (x_0, y_0), this equation modifies to (Figure 2)

$$(x_i + x_0)^2 + (y_i + y_0)^2 = r^2 . \tag{4}$$

The substitution of three known points leads to a system of three equations with the three unknowns x_0, y_0 and r. Hence, x_0, y_0 and r can be solved using

$$y_0 = \frac{1}{2}\left[\frac{(x_3^2 - x_1^2 + y_3^2 - y_1^2)(x_1 - x_2) + (x_2^2 - x_1^2 + y_2^2 - y_1^2)(x_3 - x_1)}{(x_1 - x_2)(y_1 - y_3) + (x_1 - x_3)(y_2 - y_1)}\right],$$

$$x_0 = \frac{1}{2}\frac{x_2^2 - x_1^2 + y_2^2 - y_1^2}{x_1 - x_2} + y_0\frac{y_2 - y_1}{x_1 - x_2}, \tag{5}$$

$$r = \sqrt{(x_1 - x_0)^2 + (y_1 - y_0)^2}\,.$$

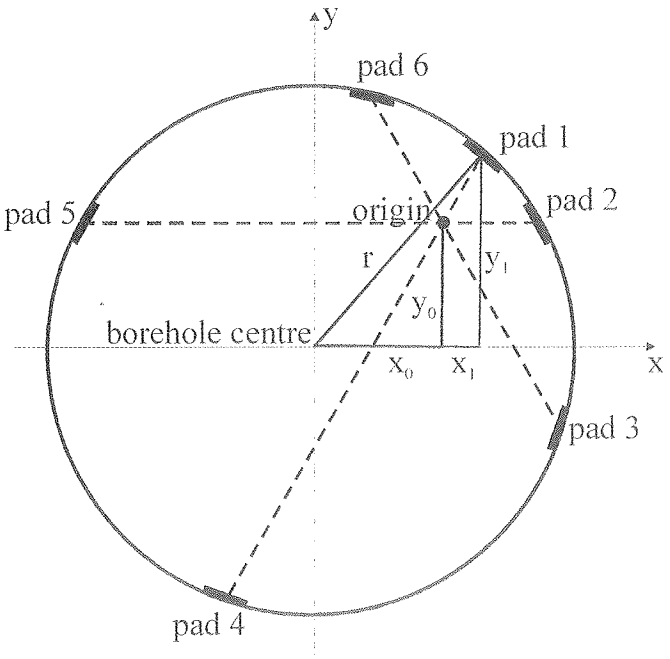

FIG. 2 Cross-section of a borehole. The tool axis is decentralized by the displacement vector (x_0, y_0). The value r can be calculated using Pythagoras theorem.

In a circular wellbore, any pad combination will always yield the shape of the borehole wall. However, for irregular borehole shapes, it is not known which combination of the pads is closest to bit size. Thus, all pad combinations are used to derive the average values of x_0 and y_0 from the circle algorithm.

Ellipse algorithm

The ellipse algorithm is particularly relevant to the interpretation of borehole breakouts (Lysne, 1986; Bässler, 1995). The breakout shape can be approximated by an ellipse with half-axes a and b. For a decentralized tool, the tool center is at (x_0, y_0) with respect to the center of the ellipse. Furthermore, the ellipse representing a breakout is rotated with respect to the x-axis (E-W direction) by an angle φ. The ellipse algorithm uses an elliptical approximation of the borehole shape and is based on a linear inversion to obtain the model parameters $\alpha, \beta, \gamma, \delta, \varepsilon$ of the ellipse, defining the vector m as

$$m^T = (\alpha \;\; \beta \;\; \gamma \;\; \delta \;\; \varepsilon). \tag{6}$$

The result of the inversion is

$$m = (G^T \cdot G)^{-1} \cdot G^T \cdot d, \tag{7}$$

with a data vector

$$d^T = (1\ 1\ 1\ 1\ 1\ 1). \tag{8}$$

The model matrix G contains the six measured data points at each depth interval. The tool position relative to the center of the ellipse can be calculated from

$$x_0 = \frac{(\beta \cdot \varepsilon - \gamma \cdot \delta)}{\det(A)} \quad \text{and} \quad y_0 = \frac{(\beta \cdot \delta - \alpha \cdot \varepsilon)}{\det(A)}, \tag{9}$$

where A is a matrix composed of the model parameters $\alpha, \beta, \gamma, \delta$ and ε (Bässler, 1995).

The ellipse algorithm provides the true center of the wellbore for both exactly elliptical and exactly circular borehole shapes because the circle is a special case of an ellipse.

Center of mass method

In the center of mass method (Barton, 1988; Bässler, 1995), the point mass objects are the pads and the 'mass' m

is considered to be equal at each pad ($m = 1$). The tool center is at (x_0, y_0) with respect to the borehole center, with the pad coordinates ($P_i \cos\theta_i$, $P_i \sin\theta_i$) (Figure 3). The center of mass is given by the equations

$$x_0 = -\frac{1}{6}\sum_{i=1}^{6} P_i \cos\theta_i \quad \text{and} \quad y_0 = -\frac{1}{6}\sum_{i=1}^{6} P_i \sin\theta_i \,. \quad (10)$$

Chord approach

Two main geometric principles are used in the chord approach:

1. The theorem of Pythagoras, stating

$$x^2 + y^2 = R^2 \,, \text{ which results in}$$
$$(x_0 + P_i \cos\theta_i)^2 + (y_0 + P_i \sin\theta_i)^2 = R^2. \quad (11)$$

2. The rule of chords, which states: If two chords of a circle intersect, the product of the segments from the first chord equals the product of the segments of the second chord. This means that the product of the length of opposite arms is constant, that is,

$$P_1 P_4 = P_2 P_5 = P_3 P_6 \text{ and equals } R^2 - (x_0^2 + y_0^2) \,. \quad (12)$$

The true center of a circular borehole can be calculated by (Appendix A)

$$x_0 = -\frac{1}{3}\sum_{i=1}^{6} P_i \cos\theta_i \quad \text{and} \quad y_0 = -\frac{1}{3}\sum_{i=1}^{6} P_i \sin\theta_i \,. \quad (13)$$

The tool offset determined by the chord approach is double the value resulting from the center of mass. Note equation (10) is exactly the half of equation (13). Hence, the center of mass method will always suggest a borehole center that is halfway between the tool position and the real tool center in circular boreholes.

COMPARISON OF TOOL DECENTRALIZATION CORRECTION TECHNIQUES ON SYNTHETIC BOREHOLE SHAPES

Methods

In circular boreholes, the circle algorithm, the ellipse algorithm and the chord approach provide the exact center of the well for decentralized tool positions, and the center of mass method exhibits a systematic offset. To interpret breakouts, these methods are tested in the following different borehole shapes:

- a circle to illustrate an in-gauge borehole,
- ellipses with different eccentricities to represent symmetric borehole breakouts (Figure 4a), and
- combinations of smaller circles intersecting bigger ones to illustrate key-seating (Figures 4b and 4c).

At least 16 different tool positions have been selected for each shape, and the synthetic caliper data have been computed using the equation of a circle or an ellipse and three lines crossing each other at a single point at 60° angles. Two different pad 1 orientations were used at each tool position (10° and 40°) with respect to the x-axis. This results in a minimum of 32 individual computations for each method in each borehole shape (Figure 4).

Results

Figure 5 shows two example configurations of an elliptical borehole shape and a big key-seat shape. To quantify the results, we calculated the distances between the calculated borehole center and the true borehole center as percentage of the borehole radius. For each individual tool position and pad orientation, the distance between the calculated offset to the true borehole center (i.e. the error) was calculated. For each shape the errors were averaged and displayed as histograms (Figure 6). Results are as follows:

- Circular wells: All techniques except the center of mass

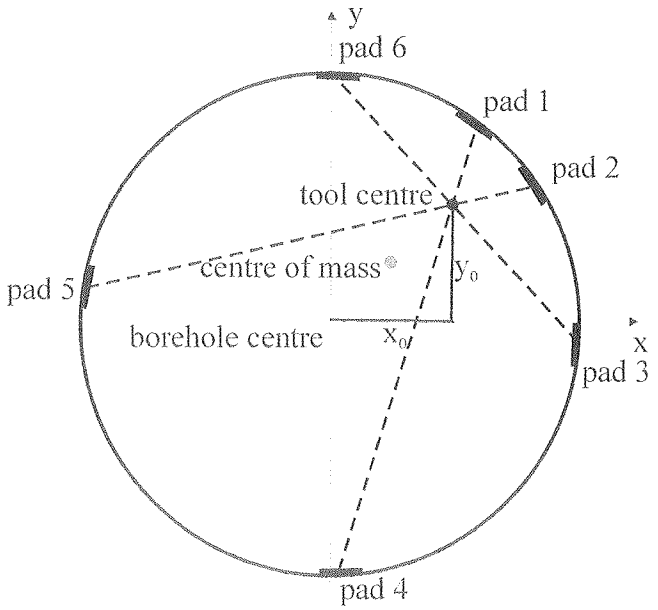

FIG. 3 Cross-section of a circular borehole with a decentralized six-arm caliper tool showing the center of mass being halfway between the tool position and the center of a circular borehole.

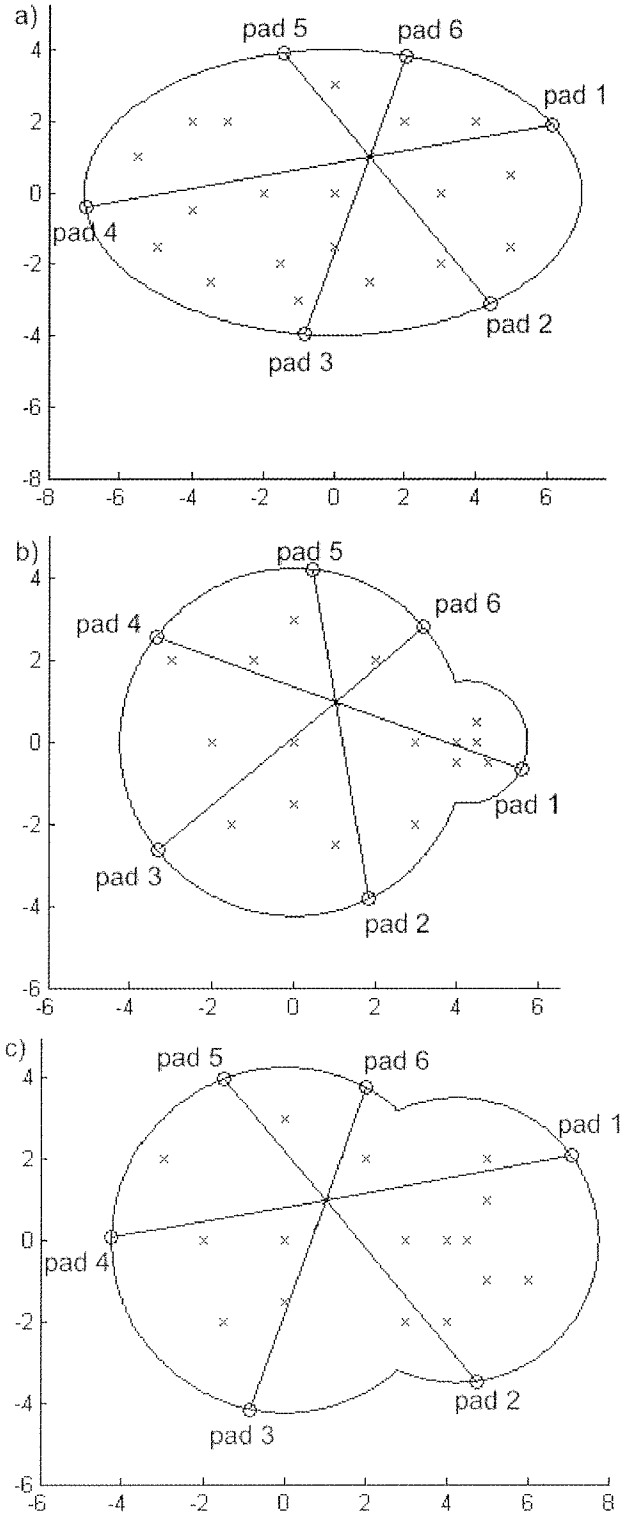

FIG. 4 Borehole shapes used to test each algorithm: a) elliptical wellbore shape (example tool rotated 10° anticlockwise), b) small key-seat (example tool rotated 40° anticlockwise), c) large key-seat (example tool rotated 10° anticlockwise). The crosses mark tested tool positions.

method give the exact center of circular boreholes. The 'center' calculated by the center of mass method is always halfway between the tool position and the center of a circular borehole (Figure 3).

- Elliptical boreholes: The ellipse algorithm precisely calculates the center of the elliptical boreholes (by definition) (Figure 6a).
- Small key-seats: The chord approach provided the best result in the modeled small key-seat scenario (Figure 6b). The circle algorithm yields a good result in small key-seats, as there are a lot of pad combinations in which none of the pads, or only one pad, lies within the key-seat (Figure 7). Hence, the overall average is close to the borehole center. It is impossible to calculate the center of the ellipse in small key-seats when the tool is strongly off-centered and at least three pads lie within the

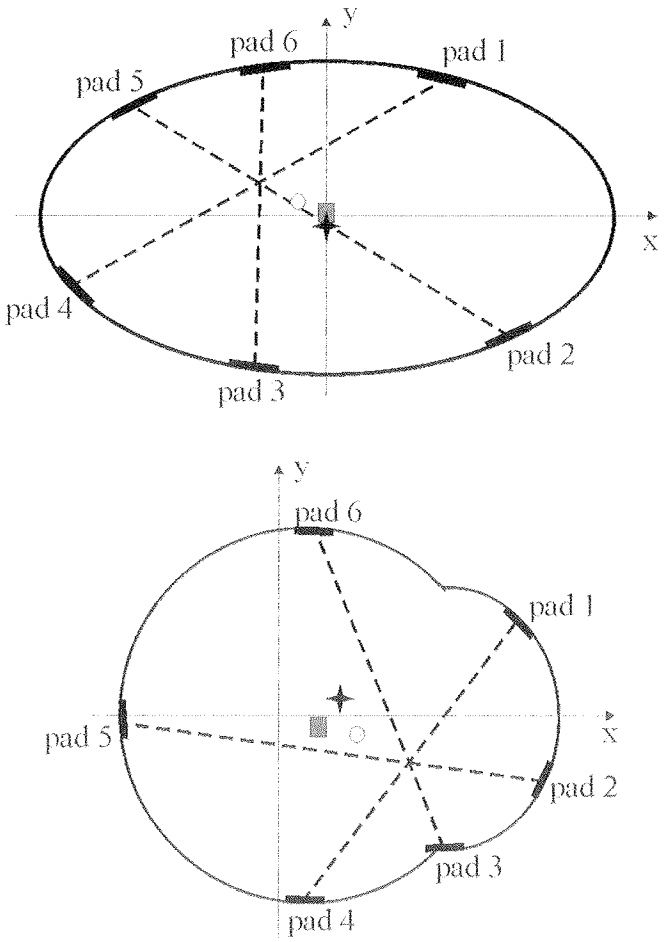

FIG. 5 Examples of off-centered tools in an elliptical borehole shape and a big key-seat shape. The circle represents the results of the center of mass method, the star represents the chord approach and the square represents the ellipse algorithm.

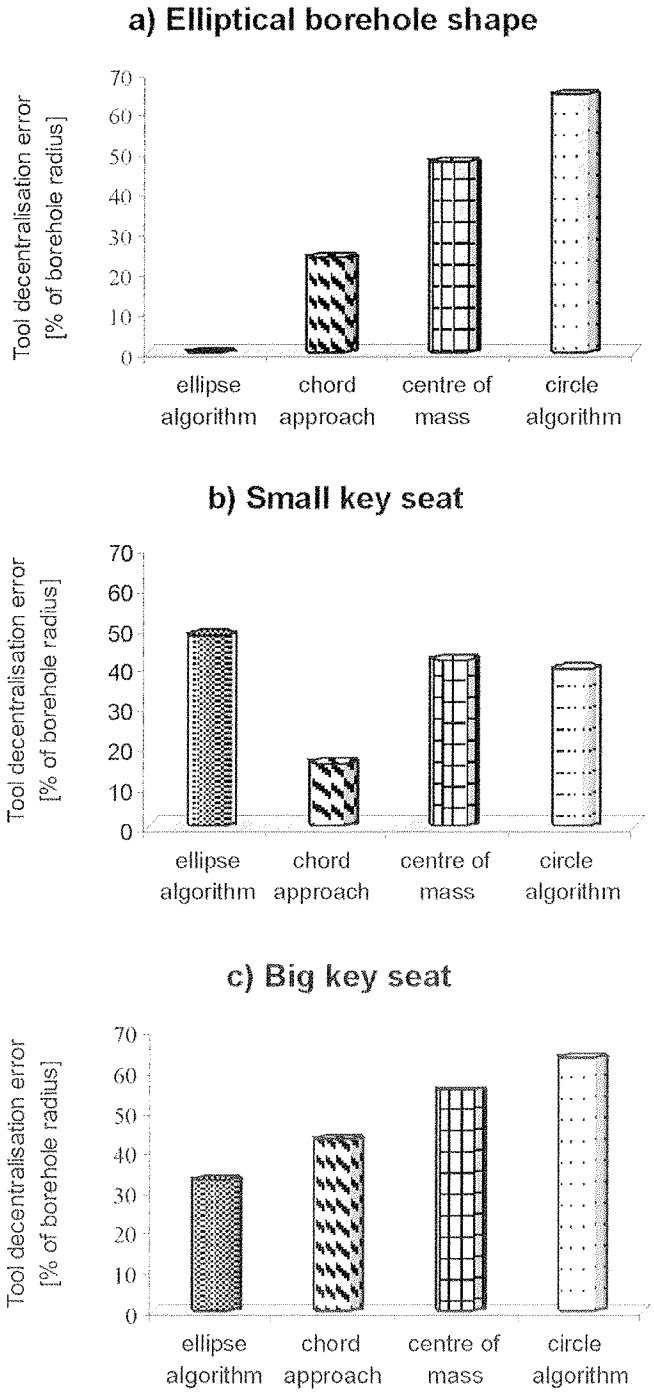

FIG. 6 Comparison of the results of all tested methods for a) elliptical borehole shape representing a breakout, b) small key-seat, and c) big key-seat.

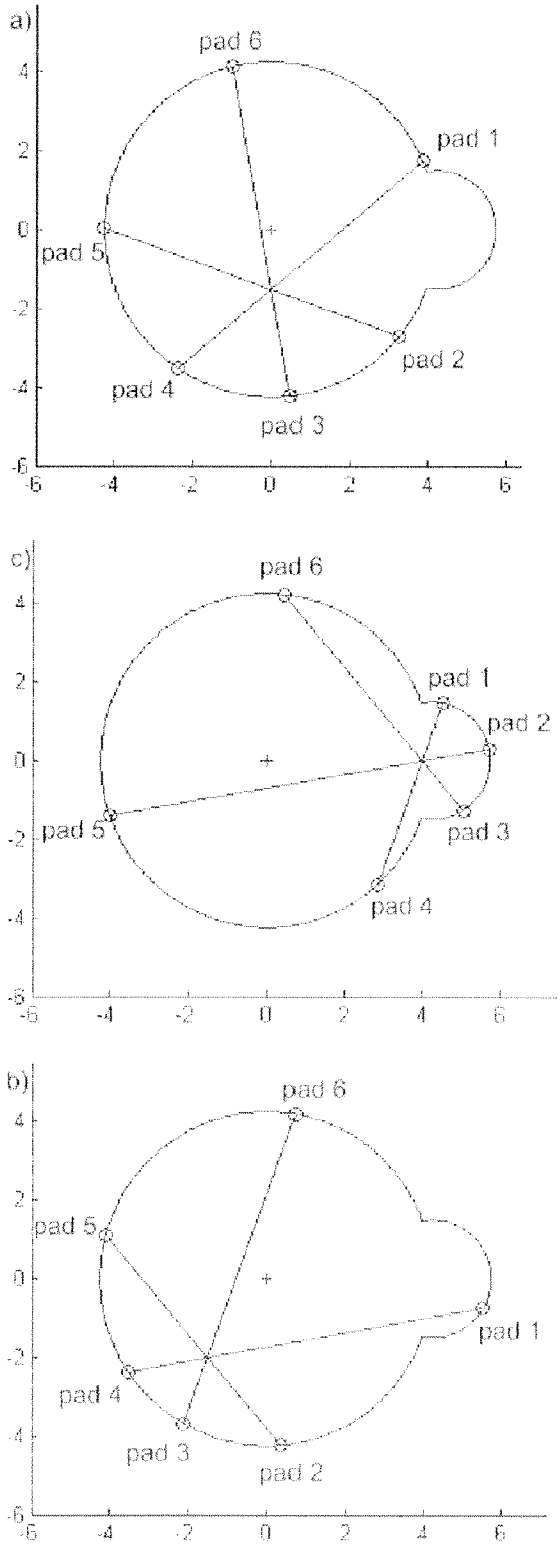

FIG. 7 Example pad orientations in the case of a small key-seat: a) none of the pads are within the key-seat, b) only one pad within the key-seat, and c) three pads within the key-seat. The cross marks the borehole center.

key-seat. Therefore, the ellipse algorithm performed poorly in the small key-seat case (Figure 6b).

- Big key-seats: The ellipse algorithm was the most precise method for calculating tool decentralization in the big key-seat scenario (Figure 6c). However, offset of the calculated center from the true center was quite large in all four methods (Figure 6c).

Recommendations

The ellipse algorithm followed by the chord approach provided the best results for all three borehole enlargement scenarios and the circular wellbores. However, the ellipse algorithm is not recommended if more than two pads are within a small key-seat. In conclusion, the ellipse algorithm and the chord approach provided the best corrections for tool decentralization. Thus, they were implemented as correction routines to correct for tool decentralization in the authors' Six Arm Caliper (SAC)-software. Both methods are implemented in the SAC-code to enable the user to switch to the chord approach if small key-seating occurs. The SAC-software enables users to create plots of pad position, relative to the borehole center, at any depth. These plots are then 'stacked' over a selected depth interval to give an impression of the borehole shape. 'Stacking' allows breakouts to be interpreted and their azimuth and width to be reliably ascertained.

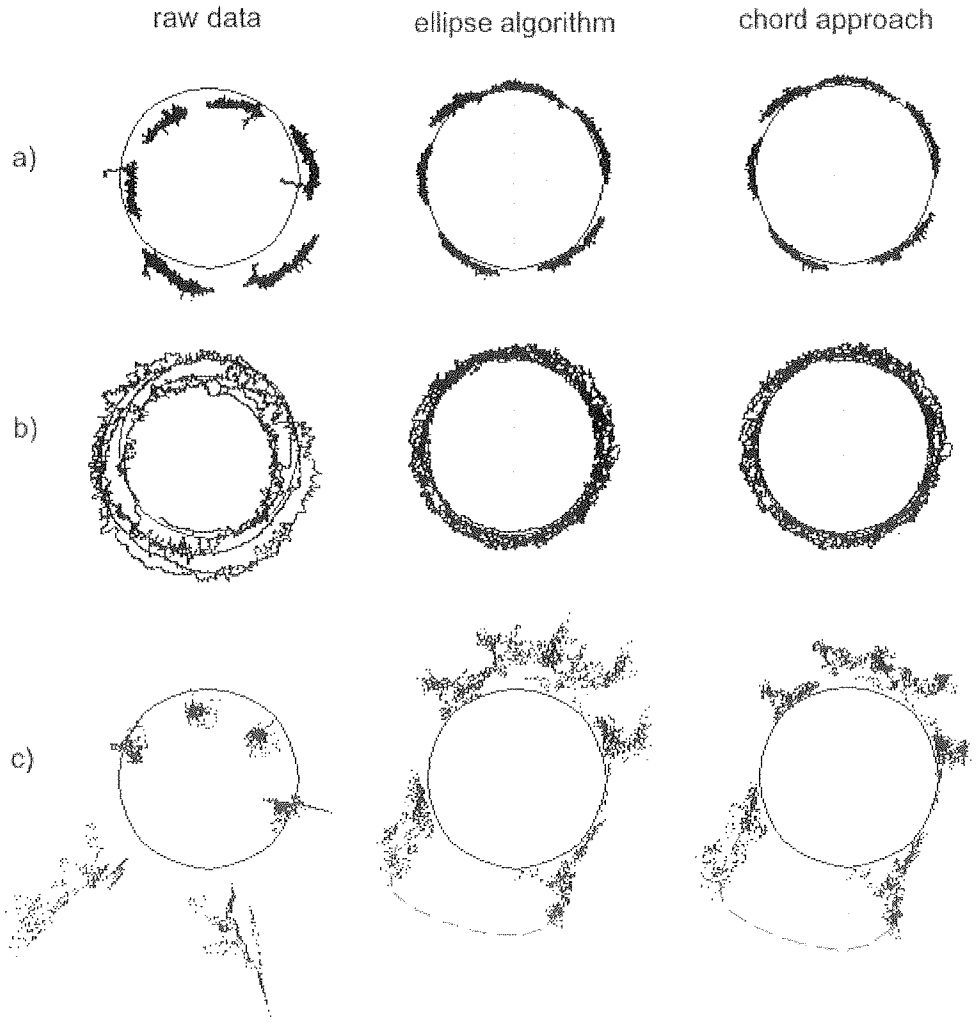

FIG. 8 Comparison of raw data contour plots and data corrected using the ellipse algorithm and the chord approach. The circle illustrates an in-gauge well (8.5 inch bit size). Note the slow rotation of the tool in Figure 8a, which only rotates 35° over the entire logging interval. The deviation of the well is 19-28°. Figure 8b shows another well with a deviation of about 13°. Figure 8c illustrates a horizontal well (deviation of 76-92°) with a large key-seat at the low side of the hole.

APPLICATION ON BOREHOLE DATA

Observed six-arm caliper data from nine wells were corrected for tool decentralization and interpreted using the SAC-software. Examples of the decentralization correction and interpretation of six-arm data from four wells are given below.

Deviated circular wells: In a circular well with a deviation between 19° and 28°, a strong tool decentralization (Figure 8a) occurred that was successfully corrected by the ellipse algorithm and the chord approach. Figure 8b illustrates an example in a well with a deviation of about 13°. Comparing the plot of the raw data and the corrected data, it is obvious that both the ellipse algorithm and the chord approach successfully correct for tool decentralization.

Big key-seat in a horizontal well: Horizontal wells commonly suffer from key-seating, and the six-arm tool becomes highly decentralized (Figure 8c). Figure 8c illustrates the improvement in the data display after the correction for tool decentralization in comparison to the stacked raw data. Both the chord approach and the ellipse algorithm provide a better visualization of the borehole shape and the interpretation of a large key-seat. The chord approach represents the circular borehole slightly better than the ellipse algorithm because several pads lie within the key-seat.

Breakouts in a near vertical well: The decentralization correction techniques were tested in a vertical well containing numerous breakouts (examples in Figure 9). Both the ellipse algorithm and the chord approach yield easily interpretable breakout orientations and widths (Figure 9).

CONCLUSIONS

An analysis of six-arm caliper data for breakouts can be performed by stacking data that has been corrected for tool decentralization. The synthetic data presented herein demonstrates that the elliptical and chord approach for decentralization corrections are most successful. The examples on observed data show the direct need for corrections because even in circular wells the decentralization effect is significantly biasing the logging data. These algorithms are successfully used to detect breakouts and key-seats on real data using the authors' SAC-program.

The ellipse and chord techniques presented herein can be used to improve other applications of six-arm caliper data, such as calculation of hole volume for casing or stratigraphic analysis. Furthermore, these techniques may be used for other six-arm tools, such as Schlumberger's EMS (Environmental Measurement Sonde) and Baker Atlas' STAR (Simultaneous Acoustic and Resistivity Imager).

ACKNOWLEDGMENTS

The authors are grateful to the following individuals and companies for providing test data and the permission to publish: Carsten Pretzschner, University of Freiberg, Christian Bücker, RWE-DEA AG, Tony Batchelor, Geoscience Limited, John Cook, Schlumberger, Jörg Baumgärtner and André Gérard, EEIG Heat-Mining, Soultz-sous-Forêts, Rob Van Eijs, Netherlands Institute of Applied Geoscience TNO. The authors also wish to thank Stephen Hickman and Richard Plumb for their insightful reviews that greatly improved this paper.

REFERENCES

Barton, C., 1988, Development of in-situ stress measurement techniques for deep drill holes: Dissertation, Stanford University, USA.

Bässler, H., 1995, Dezentrierungskorrektur von BHTV-Daten angewandt auf die Tiefbohrung VGS-Rußland und Hochauflösende Kaliberauswertung am Beispiel der KTB:

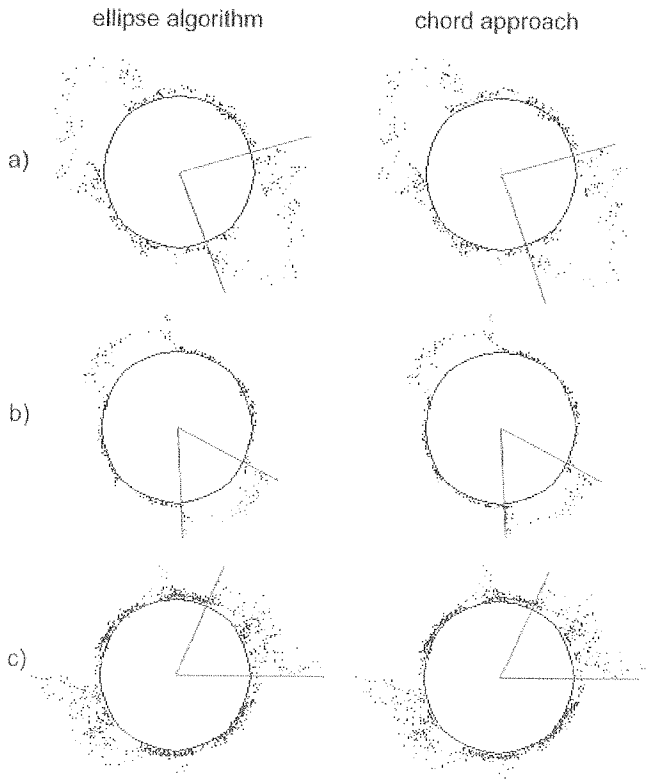

FIG. 9 Breakout examples corrected with the ellipse algorithm and the chord approach. The well had caliper log data from 2624-3157 m depth and wellbore deviations of 1.6-2°. Only slight differences in the corrections are visible. The interpreted stress direction in Figure 9a is 115°, in Figure 9b is 146° and in Figure 9c is 57°.

Geophysical Institute, University of Karlsruhe, Diploma-Thesis.

Bell, J. S., 1990, Investigating stress regimes in sedimentary basins using information from oil industry wireline logs and drilling records, *in* Hurst, A., Lovell, M., and Morton, A., eds., *Geological Applications of Wireline Logs*: Geological Society of London Special Publication, no. 48, p. 305–325.

Gough, D. I., and Bell, J. S., 1982, Stress orientations from borehole wall fractures with examples from Colorado, east Texas and northern Canada: *Canadian Journal of Earth Sciences*, vol. 19, no. 7, p. 1358–1370.

Jarosinski, M., 1998, Contemporary stress field distortion in the Polish part of the Western Outer Carpathians and their basement: *Tectonophysics*, vol. 297, issue 1-4, p. 91–119.

Kirsch, V., 1898, Die Theorie der Elastizität und die Bedürfnisse der Festigkeitslehre: *Zeitschrift des Vereines Deutscher Ingenieure*, vol. 29, July, p. 797–807.

Lysne, P., 1986, Determination of borehole shape by inversion of televiewer data: *The Log Analyst*, vol. 27, no. 3, p. 64–71.

Peska, P., and Zoback, M.D., 1995, Compressive and tensile failure of inclined wellbores and determination of in situ and rock strength: *Journal of Geophysical Research*, vol. 100, no. B7, p.12791–12811.

Plumb, R. A., and Hickman, S. H., 1985, Stress-induced borehole elongation: a comparison between the four-arm dipmeter and the borehole televiewer in the Auburn geothermal well: *Journal of Geophysical Research*, vol. 90, no. B7, p. 5513–5521.

Shlyapobersky, J., and Chudnovsky, A., 1994, Review of recent developments in fracture mechanics with petroleum engineering applications, SPE 28074, *in* SPE/ISRM Rock Mechanics in Petroleum Engineering Conference Transactions: Society of Petroleum Engineers, Delft, The Netherlands, p. 381–389.

Sibson, R. H., 1994, Crustal stress, faulting and fluid flow, *in* Parnell, J., ed., *Geofluids; Origin, Migration and Evolution of Fluids in Sedimentary Basins*: Geological Society of London Special Publication, vol. 78, p. 69–84.

Zajac, B. J., and Stock, J. M., 1997, Using borehole breakouts to constrain the complete stress tensor: Results from the Siljan Deep Drilling Project and offshore Santa Maria Basin, California: *Journal of Geophysical Research*, vol. 102, no. B5, p. 10083–10100.

APPENDIX A
THE CHORD APPROACH

The chord approach uses the measured radii and the displacement vector of the tool axis relative to the borehole center to calculate the real radius and the new angles between the pads, using the theorem of Pythagoras and the rule of chords. The azimuths of the pads are: $\theta_i = \theta - (i-1) \cdot 60°$ for $i = 1,\ldots,6$ (Figures 1 and 2).

1. According to Pythagoras,

$$P_i^2 + 2P_i\,(x_0 \cos\theta_i + y_0 \sin\theta_i) = R^2 - (x_0^2 + y_0^2), \quad \text{(A.1)}$$

2. According to the rule of chords,

$$P_i\,P_{i+3} = R^2 - (x_0^2 + y_0^2) = P_1\,P_4 = P_2\,P_5 = P_3\,P_6 \quad \text{for } i = 1, 2, 3 \quad \text{(A.2)}$$

$$\Rightarrow P_i^2 + 2P_i\,(x_0 \cos\theta_i + y_0 \sin\theta_i) = P_i\,P_{i+3} \text{ for } i = 1, 2, 3. \quad \text{(A.3)}$$

Division by P_i and multiplying by $\cos\theta_i$ (or $\sin\theta_i$ to obtain equation (A.8)) results in

$$2(x_0 \cos^2\theta_i + y_0 \sin\theta_i \cos\theta_i) = P_{i+3}\cos\theta_i - P_i \cos\theta_i,\ i=1, 2, 3. \quad \text{(A.4)}$$

Because of the validity of $\theta_{i+3} = \theta_i + 180°$ for $i = 1, 2, 3$ and with

$$\begin{aligned} &\cos\theta_{i+3} = -\cos\theta_i \Leftrightarrow \sin\theta_{i+3} = -\sin\theta_i,\\ &\cos^2\theta_{i+3} = \cos^2\theta_i \Leftrightarrow \sin^2\theta_{i+3} = \sin^2\theta_i,\\ &\sin\theta_{i+3}\cos\theta_{i+3} = \sin\theta_i \cos\theta_i\,, \end{aligned} \quad \text{(A.5)}$$

the following equation results

$$P_i \cos\theta_i + P_{i+3}\cos\theta_{i+3} = -x_0\,(\cos^2\theta_i + \cos^2\theta_{i+3}) - y_0\,(\sin\theta_i \cos\theta_i + \sin\theta_{i+3}\cos\theta_{i+3})\,, \quad \text{(A.6)}$$

$$\Rightarrow \sum_{i=1}^{6} P_i \cos\theta_i = -x_0 \sum_{i=1}^{6} \cos^2\theta_i - y_0 \sum_{i=1}^{6} \sin\theta_i \cos\theta_i\,, \quad \text{(A.7)}$$

$$\Rightarrow \sum_{i=1}^{6} P_i \sin\theta_i = -y_0 \sum_{i=1}^{6} \sin^2\theta_i - x_0 \sum_{i=1}^{6} \sin\theta_i \cos\theta_i\,. \quad \text{(A.8)}$$

With

$$\cos^2\theta = \frac{1}{2}(1 + \cos 2\theta),\ \sin^2\theta = \frac{1}{2}(1 - \sin 2\theta),$$

$$\sin\theta\cos\theta = \frac{1}{2}\sin 2\theta \text{ and } \theta_i = \theta - (i-1)60°,$$

follows

$$x_0 = -\frac{1}{3}\sum_{i=1}^{6} P_i \cos\theta_i \text{ and } y_0 = -\frac{1}{3}\sum_{i=1}^{6} P_i \sin\theta_i\,. \quad \text{(A.9)}$$

The determination of the center by the chord approach is the double of the center of weight of the (x, y) components of the individual pads.

ABOUT THE AUTHORS

Diana Wagner finished her diploma thesis in geophysics at the Geophysical Institute of the University of Karlsruhe in 2003. She worked on borehole data and developed a program to analyze and interpret oriented six-arm caliper data for stress analysis. Now she is working for the MERAMEX 3 project at the Geophysical Institute of the University of Kiel. She can be contacted at diana@geophysik.uni-kiel.de.

Birgit Müller was the vice-chair of the World Stress Map project from its inception until 1992 and has made major contributions to the European part of the World Stress Map. A major topic of her research is the analysis and interpretation of borehole data for stress analysis. She completed her PhD on borehole guided waves in 1993 from the University of Karlsruhe. She has worked for the World Stress Map project at the Heidelberg Academy of Sciences since 1995. Her main interests are the sources, transfer and concentration of tectonic stresses on reservoir to continental scales. She can be contacted at birgit.mueller@gpi.uni-karlsruhe.de.

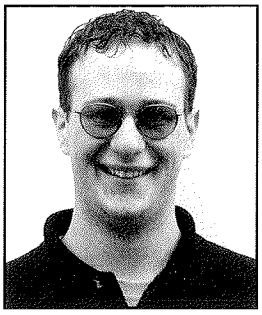

Mark Tingay received his PhD in geophysics from the University of Adelaide in 2003. He worked in the National Centre for Petroleum Geology and Geophysics at the University of Adelaide before joining the World Stress Map project at the University Karlsruhe in 2003. His main interests are petroleum geomechanics, overpressures and neotectonics. He is a member of AAPG, SEG, SPE, EAGE, ASEG and PESA. He can be contacted at mark.tingay@gpi.uni-karlsruhe.de.